

GAMMA-RAY BURSTS: NEW RULERS TO MEASURE THE UNIVERSE

GIANCARLO GHIRLANDA,¹ GABRIELE GHISELLINI,¹ DAVIDE LAZZATI,² AND CLAUDIO FIRMANI¹

Received 2004 July 27; accepted 2004 August 6; published 2004 August 18

ABSTRACT

The best measure of the universe should be done using a standard “ruler” at any redshift. Type Ia supernovae (SN Ia) probe the universe up to $z \sim 1.5$, while the cosmic microwave background (CMB) primary anisotropies concern basically $z \sim 1000$. Apparently, gamma-ray bursts (GRBs) are all but standard candles. However, their emission is collimated, and the collimation-corrected energy correlates tightly with the frequency at which most of the radiation of the prompt is emitted, as found by Ghirlanda et al. Through this correlation we can infer the burst energy accurately enough to probe the intermediate-redshift ($z < 10$) universe. Using the best known 15 GRBs we find very encouraging results that emphasize the cosmological GRB role. A combined fit with SN Ia yields $\Omega_M = 0.37 \pm 0.10$ and $\Omega_\Lambda = 0.87 \pm 0.23$. Assuming in addition a flat universe, the parameters are constrained to be $\Omega_M = 0.29 \pm 0.04$ and $\Omega_\Lambda = 0.71 \pm 0.05$. GRBs accomplish the role of “missing link” between SN Ia and CMB primary anisotropies. They can provide a new insight on the cosmic effects of dark energy, complementary to the one supplied by CMB secondary anisotropies through the integrated Sachs-Wolfe effect. The unexpected standard candle cosmological role of GRBs motivates us with the most optimistic hopes for what can be obtained when the GRB-dedicated satellite, *Swift*, is launched.

Subject headings: cosmology: observations — gamma rays: bursts

Online material: color figures

1. INTRODUCTION

Recently, Ghirlanda et al. (2004, hereafter GGL04) found a surprisingly tight correlation between the peak of the γ -ray spectrum E_{peak} (in a νF_ν plot) and the collimation-corrected energy emitted in γ -rays E_γ in long gamma-ray bursts (GRBs). The latter is related to the isotropically equivalent energy $E_{\gamma, \text{iso}}$ by the value of the jet aperture angle θ , by $E_\gamma = E_{\gamma, \text{iso}}(1 - \cos \theta)$. The scatter around this correlation is tight enough to wonder if the correlation itself can be used for a reliable estimate of $E_{\gamma, \text{iso}}$, making GRBs distance indicators and therefore probes for the determination of the cosmological (Ω_M , Ω_Λ)-parameters and for the exploration of the matter to vacuum dominance transition.

This issue is similar to the case of Type Ia supernovae (SNe Ia): they are not perfect standard candles (i.e., their luminosities are not all the same); nevertheless the luminosity of a specific supernova can be found through the correlation of their luminosity and the speed of the decay of their light curve (i.e., the slower the brighter; Phillips 1993; Riess et al. 1995). It is the existence of this correlation among SNe Ia that made possible their cosmological use (Riess et al. 2004, hereafter R04; Perlmutter et al. 1999; Schmidt et al. 1998).

Very recently, this problem has been explored by Dai et al. (2004), who found tight constraints on Ω_M and Ω_Λ using the correlation found by GGL04. Their result, however, is based on a strong assumption: they assume as universal the correlation measured in a particular cosmology (without errors on its slope) and use it to derive the cosmology itself. Actually, the best-fit luminosity depends on the cosmology adopted to derive burst luminosities, and the correlation should be recalibrated for each cosmology.

In this Letter we demonstrate that a correct approach leads to less tight constraints on the cosmological parameters using GRBs alone. On the other hand, a more interesting cosmolog-

ical result can be achieved if a combined fit with SNe Ia is performed.

2. THE HUBBLE DIAGRAM OF GRBs

As in the case of SNe Ia, the use of a class of objects as cosmological “rulers” requires that they be standard candles. The luminosity of GRBs, calculated assuming isotropy, spans ~ 4 orders of magnitude (Frail et al. 2001), but strong observational evidence (i.e., the achromatic break in the afterglow light curve) indicates that the burst emission is collimated into a cone/jet of some aperture angle θ (Levinson & Eichler 1993; Rhoads 1997; Sari et al. 1999; Fruchter et al. 1999). The corresponding energy emitted in γ -rays, corrected by the collimation factor $(1 - \cos \theta)$, clusters around $E_\gamma \sim 10^{51}$ ergs, with a small dispersion (0.5 dex), yet not small enough for a cosmological use (Bloom et al. 2003).

GGL04 found a tight correlation between E_γ and the (rest frame) peak energy E_{peak} of the νF_ν prompt emission spectrum: $E_\gamma \propto E_{\text{peak}}^x$. The exact value of x depends on the assumed cosmology. Using $\Omega_M = 0.3$ and $\Omega_\Lambda = 0.7$ we have

$$E_\gamma = (4.3 \pm 0.9) \times 10^{50} \left(\frac{E_{\text{peak}}}{267 \text{ keV}} \right)^{1.416 \pm 0.09} \text{ ergs.} \quad (1)$$

The scatter of the data points around the correlation is of the order of 0.1 dex. This allows us to reconstruct the value of E_γ by measuring E_{peak} .

This is analogous to SNe Ia, for which there is a tight relation between their peak luminosity and the stretching factor of their optical light curve (Phillips 1993; Goldhaber et al. 2001), with less luminous supernovae showing a faster postmaximum light curve decay (Riess et al. 1995). The proper modeling of this effect (Hamuy et al. 1996; Perlmutter et al. 1999) improves the determination of the SN Ia luminosity and consequently reduces the scatter in the Hubble diagram, yielding constraints on the cosmological parameters (see R04, who use SNe Ia with redshift up to $z \sim 1.75$).

¹ INAF–Osservatorio Astronomico di Brera, via Bianchi 46, 23807 Merate, Italy.

² Institute of Astronomy, Madingley Road, CB3 0HA, Cambridge, UK.

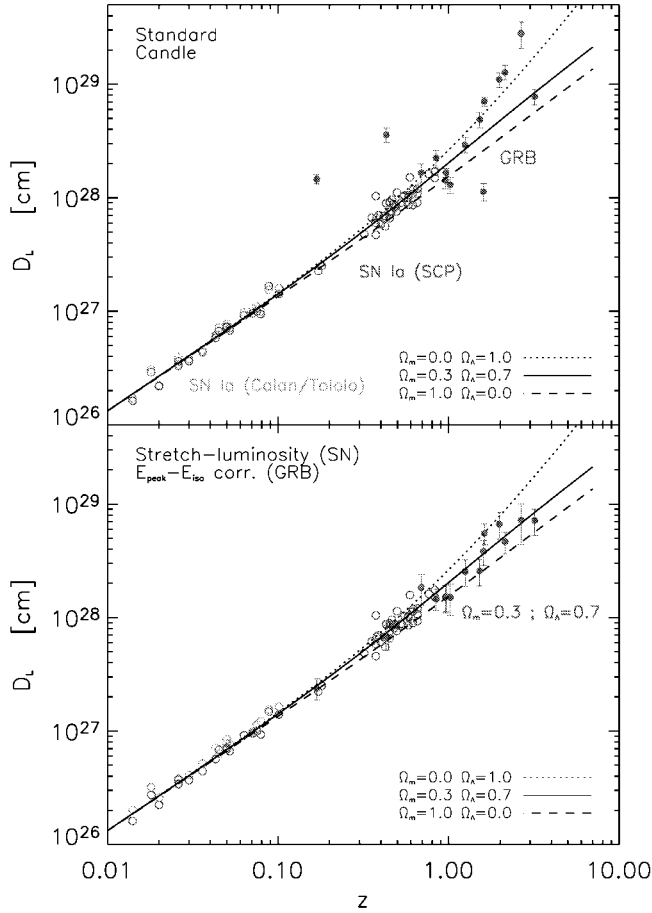


FIG. 1.—Classical Hubble diagram in the form of luminosity distance D_L vs. redshift z for SNe Ia (open circles: Calán/Tololo sample [Hamuy et al. 1996]; Supernova Cosmology Project [SCP; Perlmutter et al. 1999]) and GRBs (filled circles: the 15 bursts in GGL04). In the top panel the SNe Ia and GRBs are treated as standard candles (no corrections applied); for GRBs $E_\gamma = 10^{51}$ ergs is assumed. In the bottom panel we have applied the stretching luminosity and the E_γ - E_{peak} relations to SNe Ia and GRBs, respectively, as explained in the text. Note that for GRBs, the applied correction depends on the specific assumed cosmology: here for simplicity we assume the standard $\Omega_m = 0.3$, $\Omega_\Lambda = 0.7$ cosmology. Both panels also show different $D_L(z)$ curves, as labeled. [See the electronic edition of the Journal for a color version of this figure.]

The E_γ - E_{peak} correlation for GRBs makes them a new class of rulers for observational cosmology, and combining GRBs and SNe Ia can further reduce the region of allowed values in the cosmological parameter space. Furthermore, since GRBs are detectable at larger z , they are a powerful tool to explore in more detail the cosmic kinematics.

The difference between the standard candle assumption and the use of the intrinsic correlations, for both GRBs and SNe Ia, is shown in Figure 1 (top and bottom panel, respectively) through the Hubble diagram in the form of luminosity distance versus redshift. In the upper panel we assume that GRBs and SNe Ia are standard candles with a unique energy ($E_\gamma = 10^{51}$ ergs) for GRBs and with luminosity ($B = -21.1$) for SNe. The derivation of the luminosity distance D_L for SN follows straightforwardly from their distance modulus (R04). For GRBs we have $D_L \equiv (1+z)E_\gamma/[4\pi\mathcal{F}_\gamma(1-\cos\theta)]$, where \mathcal{F}_γ is the γ -ray fluence (i.e., the time-integrated γ -ray flux). Note that the determination of θ requires the knowledge of the isotropic energy (see, e.g., eq. [1] in Frail et al. 2001), in turn requiring specific values of $(\Omega_m, \Omega_\Lambda)$. In the bottom panel we plot SNe Ia and GRBs after correcting for the stretching luminosity and

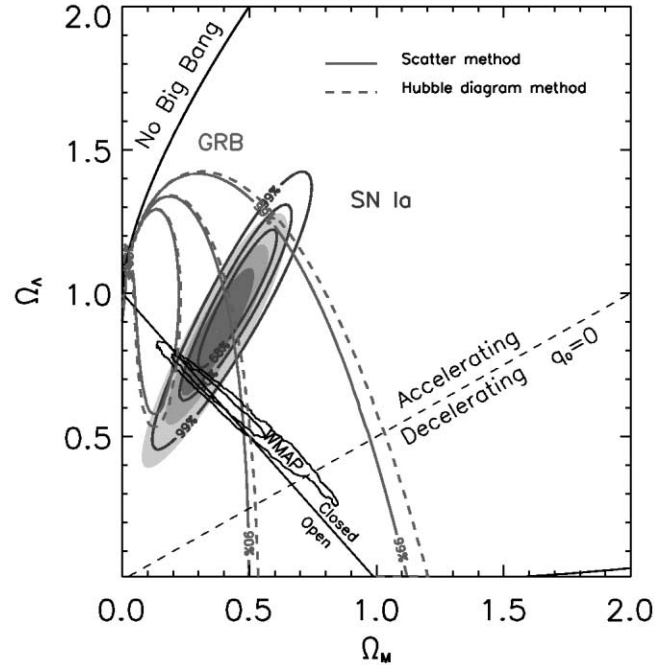


FIG. 2.—Constraints on the Ω_m - Ω_Λ plane derived for our GRB sample (15 objects, solid and dashed curves); the “gold” SN Ia sample of R04 (156 objects, contours, derived assuming a fixed value of $H_0 = 65 \text{ km s}^{-1} \text{ Mpc}^{-1}$, making the contours slightly different from Fig. 8 of R04). The WMAP satellite constraints (black contours; Spergel et al. 2003) are also shown. The three shaded ellipses are the confidence regions (dark gray: 68%; gray: 90%; light gray: 99%) for the combined fit of SNe Ia and our GRB sample. For GRBs only, the minimum $\chi^2_{\text{red}} = 1.04$ is at $\Omega_m = 0.07$, $\Omega_\Lambda = 1.2$. [See the electronic edition of the Journal for a color version of this figure.]

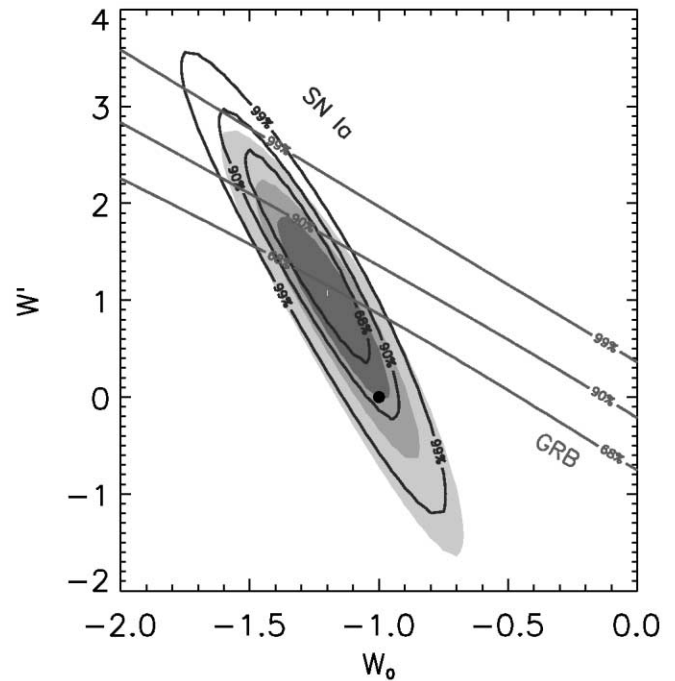


FIG. 3.—Constraints on the (w_0, w') -parameters entering the equation of state $p = (w_0 + w'z)\rho c^2$, where ρ is the dark energy density; $w_0 = -1$ and $w' = 0$ correspond to the cosmological constant Ω_Λ . We assume a flat geometry and $\Omega_m = 0.27$ (see also R04). Contours: Constraints from SNe Ia (R04). Solid diagonal lines: Constraints from our GRBs. Shaded regions: Combined constraints (dark gray, gray, and light gray for the 68%, 90%, and 99% confidence levels, respectively). [See the electronic edition of the Journal for a color version of this figure.]

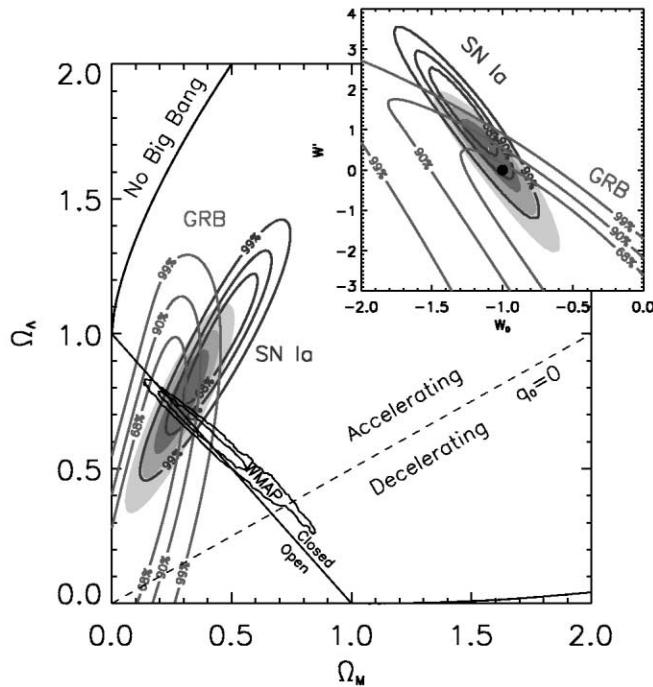


FIG. 4.—Example of how GRBs can contribute to the determination of the cosmological parameters once the E_γ - E_{peak} correlation will be found in a cosmology-independent way (i.e., finding bursts at small redshifts). For this example we assume that the correlation of eq. (1) is valid for any cosmological parameter. We show the contours in both the $(\Omega_M, \Omega_\Lambda)$ -plane (main figure) and the w_0 - w' plane (inset; a flat cosmology with $\Omega_M = 0.27$ is assumed). Lines and colors are as in Figs. 2 and 3. [See the electronic edition of the Journal for a color version of this figure.]

the E_γ - E_{peak} relations, respectively. In this case the isotropic energy $E_{\gamma, \text{iso}}$ of GRBs has been estimated from their measured E_{peak} through the E_γ - E_{peak} correlation, and the error on the slope of this correlation has been properly included in the D_L total uncertainty. Also in this case we must fix a given $(\Omega_M, \Omega_\Lambda)$ -cosmology both for the derivation of θ and for finding the best E_γ - E_{peak} relation. As in the SN Ia case, the luminosity distance of GRBs derived from their E_γ - E_{peak} correlation (bottom panel) highly reduces the scatter around the possibly different cosmologies (solid, dashed, and dotted lines). Moreover, GRBs populate the $z > 1$ region, where $D_L(z)$ is rather sensitive on $(\Omega_M, \Omega_\Lambda)$.

3. CONSTRAINTS ON COSMOLOGICAL PARAMETERS

The correlation found by GGL04 assumes $\Omega_M = 0.3$, $\Omega_\Lambda = 0.7$, and $h = 0.7$. Changes in Ω_M and Ω_Λ induce a change in the normalization and slope of equation (1), together with a different scatter of the data points around the best-fit line. What is the pair of cosmological values $(\Omega_M, \Omega_\Lambda)$ that produces the “minimum scatter” around the fit, performed using the very same $(\Omega_M, \Omega_\Lambda)$ -pair? To answer this question, we use all the 15 bursts of known redshifts, E_{peak} , and jet break time t_{break} listed in Tables 1 and 2 of GGL04. The difference with the study of Dai et al. (2004) lies mainly in that they assumed that the E_γ - E_{peak} correlation is exact and cosmology-independent when in fact it is not.³

³ For instance, using $\Omega_M = 0.4$, $\Omega_\Lambda = 0.6$ results in $E_\gamma = (3.7 \pm 0.9) \times 10^{50} (E_{\text{peak}}/267 \text{ keV})^{1.38 \pm 0.09}$ ergs (i.e., an $\sim 2.6\%$ and $\sim 16\%$ change in slope and normalization with respect to eq. [1]). With $\Omega_M = 1$, $\Omega_\Lambda = 1$ we obtain $E_\gamma = (3.0 \pm 0.9) \times 10^{50} (E_{\text{peak}}/267 \text{ keV})^{1.29 \pm 0.08}$ ergs (i.e., an $\sim 9\%$ and $\sim 30\%$ change in slope and normalization with respect to eq. [1]).

Additional differences concern (1) the estimate of the errors in the density of the interstellar medium when it is unknown (they assume $n = 3 \pm 0.33 \text{ cm}^{-3}$, while we allow n to cover the entire $1\text{--}10 \text{ cm}^{-3}$ range); (2) we do not exclude GRB 990510 and GRB 030226 from the analysis; (3) we include GRB 030429, for which a jet break time was recently found by Jakobsson et al. (2004); and (4) we always use $(1 - \cos \theta)$ (instead of the $\theta^2/2$ approximation) as the collimation correction factor (also when estimating the error in E_γ).

We also consider the 156 SNe Ia of the “gold” sample of R04 and find the corresponding $(\Omega_M, \Omega_\Lambda)$ -contours using the distance moduli and corresponding errors listed in their Table 5. Figure 2 shows our results. GRBs alone are almost insensitive to Ω_Λ but limit Ω_M to lie within ~ 0.05 and 0.22 (68% confidence level).

We also show the region pinpointed by the *Wilkinson Microwave Anisotropy Probe* (WMAP) experiment (Spergel et al. 2003), which is only marginally consistent with the allowed region from SNe Ia alone (Fig. 2). The combined GRB+SN Ia fit (filled regions in Fig. 2) selects a region that is more consistent with the cosmic microwave background results. The minimum (with a reduced $\chi^2_{\text{red}} = 1.146$) is for $\Omega_M = 0.37 \pm 0.15$ and $\Omega_\Lambda = 0.87 \pm 0.23$ (1 σ). Assuming a flat universe yields $\Omega_M = 0.29 \pm 0.04$ and $\Omega_\Lambda = 0.71 \pm 0.05$.

If we use the “classical” Hubble diagram method, we compare the D_L values given by estimating E_γ through the actual correlation found in each point of the $(\Omega_M, \Omega_\Lambda)$ -plane with the luminosity distance calculated through, e.g., equation (11) of R04 (see also Carroll et al. 1992). Then, by χ^2 statistics, we find the confidence regions in the $(\Omega_M, \Omega_\Lambda)$ -plane, which are plotted as dashed line on Figure 2. This classical method is very similar to the previous one since it uses the same available information. The small difference (contours slightly larger) is due to the fact that with the minimum scatter method, we calculate the distance of the data points from the correlation (i.e., perpendicular to the fitting line) while, using the classical Hubble diagram method, we are using the distance between the E_γ data point and the corresponding E_γ by the correlation.

We can further constrain, with the combined GRB and SN samples, the dark energy component that is parameterized by its equation of state $P = w\rho c^2$. Furthermore, w could be varying, and one possible parameterization is $w = w_0 + w'z$ (see, e.g., R04). Adopting this law, we compute the luminosity distance according to equation (14) of R04, assuming a flat cosmology with $\Omega_M = 0.27$. In this case the fit is performed in the w_0 - w' plane for GRBs, SNe, and the combined samples. As before, we recompute the E_γ - E_{peak} relation for each (w_0, w') -pair.⁴ Figure 3 reports the corresponding confidence intervals. Besides making the confidence region smaller than what was derived for SNe alone, the effect of GRBs is to include within the 68% contour of the joint SN+GRB sample (filled region) the $w_0 = -1$, $w' = 0$ point, corresponding to the classical cosmological constant.

4. DISCUSSION

GRBs can now be used as cosmological rulers, bridging the gap between the relatively nearby Type Ia supernovae and the cosmic microwave background. The *Swift* satellite (Gehrels et al. 2004), designed for the fast localization of GRBs, is ex-

⁴ As an example of how the correlation is sensitive to the change of (w_0, w') , consider that for $w_0 = -0.7$ and $w' = 0.2$, the correlation becomes $E_\gamma = (3.75 \pm 0.90) \times 10^{50} (E_{\text{peak}}/267 \text{ keV})^{1.37 \pm 0.09}$ ergs (i.e., an $\sim 3.4\%$ and $\sim 15\%$ change in slope and normalization with respect to eq. [1]).

pected to find about 100 GRBs per year: it can open up a new era for the accurate measurements of the geometry and kinematics of our universe (C. Firmani et al. 2004, in preparation). We stress that, besides finding high-redshift bursts, which are of course very important for finding tighter constraints, it is crucial to find *low-redshift* GRBs, to determine the E_γ - E_{peak} correlation in a redshift range that is not affected by the $(\Omega_M, \Omega_\Lambda)$ -values. This would allow one to use the resulting correlation unchanged for all values of $(\Omega_M, \Omega_\Lambda)$, strongly reducing the associated errors. In turn, this will allow one to constrain cosmological parameters independently from SNe Ia. This is important since GRBs are unaffected by dust extinction, and it is very unlikely that two completely different classes of objects would have similar evolutions to mimic a consistent set of cosmological parameters.

In Figure 4 we show an illustrative example of what can be done *if a given correlation were known to be valid indepen-*

dently of the cosmological parameters. For this we have chosen the correlation given by equation (1). It can be seen that even the limited sample of our bursts can strongly influence the GRB+SN confidence contours, making them more in agreement with the *WMAP* results (not unexpectedly, since we have used just the correlation appropriate for $\Omega_M = 0.3$ and $\Omega_\Lambda = 0.7$). A similar consideration concerns the Dai et al. (2004) result. We would like to stress that in order to use GRBs to find the cosmological parameters, we need a set of well-measured data, and especially a well-measured jet break time t_{break} , necessary to find the collimation angle θ , and a good spectral determination of the prompt emission.

We thank Annalisa Celotti for useful discussions. D. L. thanks the Osservatorio Astronomico di Brera for their kind hospitality during part of the preparation for this work. G. Ghirlanda thanks the MIUR for COFIN grant 2003020775_002.

REFERENCES

- Bloom, J. S., Frail, D. A., & Kulkarni, S. R. 2003, *ApJ*, 594, 674
 Carroll, S. M., Press, W. H., & Turner, E. L. 1992, *ARA&A*, 30, 499
 Dai, Z. G., Liang, E. W., & Xu, D. 2004, *ApJL*, 612, in press (astro-ph/0407497)
 Frail, D. A., et al. 2001, *ApJ*, 562, L55
 Fruchter, A. S., et al. 1999, *ApJ*, 519, L13
 Gehrels, N., et al. 2004, *ApJ*, 611, 1005
 Ghirlanda, G., Ghisellini, G., & Lazzati, D. 2004, *ApJ*, in press (astro-ph/0405602) (GGL04)
 Goldhaber, G., et al. 2001, *ApJ*, 558, 359
 Hamuy, M., Phillips, M. M., Suntzeff, N. B., Schommer, R. A., Maza, J., & Aviles, R. 1996, *AJ*, 112, 2398
 Jakobsson, P., et al. 2004, *A&A*, submitted (astro-ph/0407439)
 Levinson, A., & Eichler, D. 1993, *ApJ*, 418, 386
 Perlmutter, S., et al. 1999, *ApJ*, 517, 565
 Phillips, M. M. 1993, *ApJ*, 413, L105
 Riess, A. G., Press, W. H., & Kirshner, R. P. 1995, *ApJ*, 438, L17
 Riess, A. G., et al. 2004, *ApJ*, 607, 665 (R04)
 Rhoads, J. E. 1997, *ApJ*, 487, L1
 Sari, R., Piran, T., & Halpern, J. 1999, *ApJ*, 524, L43
 Schmidt, B. P., et al. 1998, *ApJ*, 507, 46
 Spergel, D. N., et al. 2003, *ApJS*, 148, 175